# Sensitive detection of formaldehyde using an interband cascade laser near 3.6 µm

Wei Ren<sup>a,\*</sup>, Longqiang Luo<sup>b</sup>, Frank K. Tittel<sup>b</sup>

<sup>a</sup>The Chinese University of Hong Kong, Department of Mechanical and Automation Engineering, New Territories, Hong Kong

<sup>b</sup>Rice University, Department of Electrical & Computer Engineering, 6100 Main St., Houston, TX 77005, USA

\*Tel: +852 3943 9486, E-mail: renwei@mae.cuhk.edu.hk

#### **Abstract**

We report the development of a formaldehyde ( $H_2CO$ ) trace gas sensor using a continuous wave (CW), thermoelectrically-cooled (TEC), distributed-feedback interband cascade laser (DFB-ICL) at 3.6 µm. Wavelength modulation spectroscopy was used to detect the second harmonic spectra of a strong  $H_2CO$  absorption feature centered at 2778.5 cm<sup>-1</sup> (3599 nm) in its  $v_1$  fundamental vibrational band. A compact and novel multipass cell (7.6 cm physical length and 32 ml sampling volume) was implemented to achieve an effective optical path length of 3.75 m. A minimum detection limit of 6 parts per billion (ppb) at an optimum gas pressure of 200 Torr was achieved with a 1 s data acquisition time. An Allan-Werle deviation analysis was performed to investigate the long-term stability of the sensor system and a 1.5 ppb minimum detectable concentration could be achieved by averaging up to 140 s. Absorption interference eeffects from atmospheric  $H_2O$  (2%) and  $CH_4$ (5 ppm) were also analyzed in this work and proved to be insignificant for the current sensor configuration.

#### 1. Introduction

Formaldehyde ( $H_2CO$ ) is a colorless, pungent-smelling gas that plays an important role in tropospheric chemistry [1]. Primary  $H_2CO$  sources include vehicle exhaust and fugitive industrial emissions, while secondary  $H_2CO$  is produced mainly from the breakdown of primary volatile organic compounds (VOCs) via photochemical oxidation [2,3].  $H_2CO$  is one of the most abundant gas-phase carbonyls in the atmosphere and can reach concentration levels in excess of 40 parts per billion (ppb) in polluted, urban environments [2,3]. The main loss processes include photolysis by ultraviolet (UV) radiation [4] and oxidation reaction with the OH radical to form HCO, H, and CO [1,5]. These radicals undergo further reactions to form  $HO_2$ , contributing to ozone ( $O_3$ ) formation in the presence of  $NO_3$  ( $NO_3$  and  $NO_3$ ) [3]. Precise measurements of  $H_2CO_3$  concentrations are critical to the complete understanding of  $HO_3$  ( $OH_3$  and  $OH_3$ ) chemistry and  $OH_3$  formation.

In the manufacturing industry, H<sub>2</sub>CO is frequently used as a substitute for adhesives such as ureaformaldehyde (UF) and phenol-formaldehyde (PF) resins. H<sub>2</sub>CO reagents are widely applied in fabricating furniture and decorating houses. Hence, H<sub>2</sub>CO is considered as one of the most serious indoor contaminating trace gases present in new homes. H<sub>2</sub>CO has been classified as carcinogenic to humans by the International Agency for Research on Cancer (IARC) since 2004. Numerous governmental agencies have also set reference values for the exposure to H<sub>2</sub>CO, for example the World Health Organization (WHO) specified that the concentration of H<sub>2</sub>CO in residential indoor areas must not exceed 82 ppb for 30 min [6]. Hence accurate measurements and control of  $H_2CO$  con-centration levels in indoor area are of great importance to reduce its effect on human health. In addition,  $H_2CO$  has also been identified as a potential biomarker in breath analysis of humans. For instance, in exhaled breath from breast cancer patients,  $H_2CO$  concentration levels of  $\sim$ 1.2 ppm were observed compared to normal levels of tens of ppb [7]. A sensitive and reliable human breath  $H_2CO$  analyzer can provide a promising method for noninvasive, real-time, and point-of-care disease diagnostics and metabolic status monitoring.

Many methods have been explored to detect  $H_2CO$  concentrations. Indoor  $H_2CO$  detection was investigated by analyzing samples using high-performance liquid chromatography (HPLC) [8] and gas chromatography (GC) [9]. HPLC and GC can provide ppb to sub-ppb detection sensitivity, but are not suitable for field deployment due to their weight, size and long measurement times. Semiconductor gas sensors based on gas-sensitive films provide a good alternative for  $H_2CO$  monitoring due to their low cost and short response time [10–12]. However, the selectivity of such sensors is a limitation in addition to their relatively high detection limits (>300 ppb). Electrochemical  $H_2CO$  sensors have good sensitivity and selectivity, but are limited by their poor temporal stability (time response of hour) [13,14]. Hence, there exists a need for the development of highly sensitive, selective, fast and compact  $H_2CO$  analyzers.

Laser-based spectroscopic sensors can satisfy these requirements for accurate and sensitive trace gas measurements. Direct, in situ detection of atmospheric H<sub>2</sub>CO via laser induced fluorescence (LIF) in a White-type multipass cell was reported with a minimum detection limit (MDL) of  $\sim$ 0.051 ppb in a 1 s sampling time [15]. In this sensor system, the laser pulse centered at 353.373 nm was generated by a frequency-doubled Ti:Sapphire laser (3 kHz, 0.52 W), which was pumped by a Q-switched, doubled Nd:YAG laser (532 nm, 2.89 W). Davenport et al. [16] described a simple method for H<sub>2</sub>CO detection using low resolution non-dispersive UV absorption spectroscopy. In this method, a 340-nmUV LED was collimated into a 195-mm gas cell to achieve a MDLof  $\sim$ 6.6 ppm with a response time of 20 s. A cantilever enhanced photoacoustic spectrometer was developed to measure H<sub>2</sub>CO from 1772 to 1777 cm<sup>-1</sup> using a mid-infrared quantum cascade laser (QCL) [17]. By detecting an absorption line at 1773.96 cm<sup>-1</sup> (5637 nm), the MDL and the normalized noise equivalent absorption (NNEA) coefficient using wavelength modulation were 1.3 ppb and  $6.04 \times 10^{-10} \, \mathrm{W \ cm^{-1} \ Hz^{-1/2}}$ , respectively. Tunable diode laser absorption spectroscopy (TDLAS) based H<sub>2</sub>CO sensor development and its application for atmospheric monitoring have been pioneered by Tittel et al. using difference frequency generation (DFG) based laser sources to detect the H<sub>2</sub>CO transitions centered at 2861.72 cm<sup>-1</sup> (3494 nm) or 2831.64 cm<sup>-1</sup> (3531 nm) [18–21]. Similar TDLAS systems using a multipass cell ( $\sim$ 100 m path length) developed by Fried et al. [22] and Wert et al. [23] indicated H<sub>2</sub>CO MDLs of 30–50 ppt for 1 min of averaging during airborne operation. Miller et al. [24] reported the integration of off-axis integrated cavity output spectroscopy (OA-ICOS) with an interband cascade laser (ICL) to achieve a MDL of 150 ppb H<sub>2</sub>CO. The ICL, mounted in a liquid-nitrogen cryostat emitted powers of up to 12 mW and could be tuned from 2831.8 to 2833.7 cm  $^{-1}$  ( $\sim$ 3.53  $\mu$ m) by varying the laser injection current. Recently in 2012, a room-temperature distributed feedback ICL emitting around 3493 nm was utilized by Lundqvist et al. [25] for H₂CO sensing to obtain a resolution limit of 1 ppm  $\times$  m assuming a relative absorption of 10<sup>-3</sup>. More recently in 2013, the application of optical feedback-cavity enhanced absorption spectroscopy for H₂CO trace gas analysis was reported by employing a QCL at 1769 cm<sup>-1</sup> (5653 nm) to achieve a minimum detectable H₂CO mixing ratio of 60 ppt at 10 Hz [26]. The sensor response time of 3 s was limited mainly by the sample exchange rate for a 20-sccm flow and 50-mBar sample pressure in a 20-cc sample volume.

We report here a novel  $H_2CO$  absorption sensor by taking advantages of two recent technological advances of CW, thermoelectrically-cooled (TEC), DFB 3.6  $\mu$ m ICLs, and a compact multipass gas cell. The 3.6  $\mu$ m spectral region corresponds to the strongest  $H_2CO$  infrared bands of  $v_1$  band centered at 2782.4575 cm<sup>-1</sup> (symmetric C-H stretch) and  $v_5$  band centered at 2843.9685 cm<sup>-1</sup> (asymmetric C-H stretch), respectively [27]. The sensor provides a detection sensitivity of 6 ppb at 1 s sampling time. The compact design and low power consumption make this sensor easy to deploy in stationary, mobile and airborne field applications.

### 2. Spectroscopic methodology and sensor configuration

#### 2.1 Fundamentals of laser absorption spectroscopy

Laser-based absorption spectroscopy is a widely applied technique for many gas sensing measurements due to its fast time response and quantitative nature. In particular, wavelength modulation spectroscopy (WMS) which is an extension of direct absorption spectroscopy has been used extensively for sensitive gas detection. The fundamental theory of laser based absorption spectroscopy is well understood [28–32] and is therefore only described briefly to clarify the notation and units used in this paper. The laser radiation with narrow spectral bandwidth is normally utilized for line-of-sight absorption measurements. When the laser radiation at a wavelength  $\nu$  passes through a uniform gas medium, the wavelength-dependent transmission  $\tau_{\nu}$  is determined by Beer's law:

$$\tau_{\nu} = \left(\frac{I_t}{I_0}\right)_{\nu} = \exp(-SPx\phi_{\nu}L),\tag{1}$$

where  $I_0$  and  $I_t$  are incident and transmitted radiation intensity, respectively; S (cm<sup>-2</sup> atm<sup>-1</sup>) is the line-strength of the specific transition, P (atm) the total gas pressure, x the mole fraction of the absorbing species,  $\varphi_V$  (cm) the line-shape function and L (cm) the optical path length. The line-shape function  $\varphi_V$  is usually approximated using a Voigt profile characterized by the collision-broadened full-width at half maximum (FWHM) and Doppler FWHM.

In TDLAS measurements, the laser wavelength is normally scanned across the absorption features by applying a slow (Hz) saw-tooth signal to the laser injection current. The WMS method applies an additional fast (kHz) sinusoidal modulation (at frequency f) to the laser current. The modulated absorption signal, detected by means of a photodiode, is then processed using a lock-in amplifier to demodulate the signal at the fundamental modulation frequency (f) or its harmonics (2f, 3f, etc.). For one sawtooth period, the incident laser wavelength v(t) and intensity  $I_0(t)$  are modulated and can be described by Eqs. (2) and (3) [30]:

$$v(t) = \bar{v}_0 + a\cos(2\pi f t),\tag{2}$$

$$I_0(t) = \bar{I}_0 \left[ 1 + \sum_{m=1}^{\infty} i_m \cos(m \cdot 2\pi f t + \varphi_m) \right],$$

(3)

where  $\bar{v}_0$  (cm<sup>-1</sup>) is the mean laser wavelength of the laser under modulation, a (cm<sup>-1</sup>) the modulation depth,  $\bar{I}_0$  the average laser intensity,  $i_m$  the mth Fourier coefficient of the laser intensity, and  $\varphi_m$  the initial phase of the mth order intensity modulation. Previous experimental characterization of commercial diode lasers showed that the laser intensity modulation can be described by a combination of the first two terms (m = 1, 2) [32]. Hence, the detector signal (D) which is a periodic function with a period of 1/f, can be expanded into a Fourier series expressed by Eq. (4):

$$D(t) = I_0(t)\tau(t) = \bar{I}_0[1 + i_1\cos(2\pi f t + \phi_1) + i_2\cos(2\times 2\pi f t + \phi_2)] \times \left[\sum_{k=0}^{\infty} H_k\cos(k\cdot 2\pi f t)\right],$$
(4)

where  $H_k$  is the kth order Fourier coefficient as discussed in references [31,32]. The harmonics of the detected laser intensity can be extracted by lock-in amplifier with a bandwidth determined by the low-pass filters. The case of k = 2 is generally of the highest interest in WMS, since the second harmonic signal (2f) is closely related to the absorption and is background free. In this case, the lock-in amplifier functions by multiplying the detector signal with the reference sinusoid at 2f, and shifting the harmonic component to DC. A low-pass filter is then applied to isolate the DC value and eliminate all other components such as laser and electronic noises outside the filter bandwidth, making WMS particularly useful for probing pressure broadened and overlapping absorption features.

#### 2.2 ICL characterization

 $H_2CO$  has its fundamental vibrational band with the C-H symmetric ( $v_1$ ) stretching mode at 2782 cm<sup>-1</sup> [27,33]. Several laser-based  $H_2CO$  sensors [34–36] have already been reported by detecting this absorption band. Absorption spectra based on the HITRAN database [37] are computed for standard air (i.e., 1.86%  $H_2O$ , 327 ppm  $CO_2$ , 30 ppb  $O_3$ , 320 ppb  $N_2O$ , 150 ppb CO, 1.68 ppm  $CH_4$ , 20.7%  $O_2$ , and 77.4%  $N_2$ ) mixed with 10 ppb  $H_2CO$ , to identify the optimal  $H_2CO$  transitions. Considering the possible absorption interference from ambient air (i.e.,  $H_2O$ ,  $CO_2$ ,  $O_3$ ,  $N_2O$  and  $CH_4$ ) and the commercial availability of ICL sources in this wavelength range, two optimal diagnostic windows at ~2778 and ~2781 cm<sup>-1</sup> are identified in this work for  $H_2CO$  detection; see Fig. 1 for the spectral simulation.

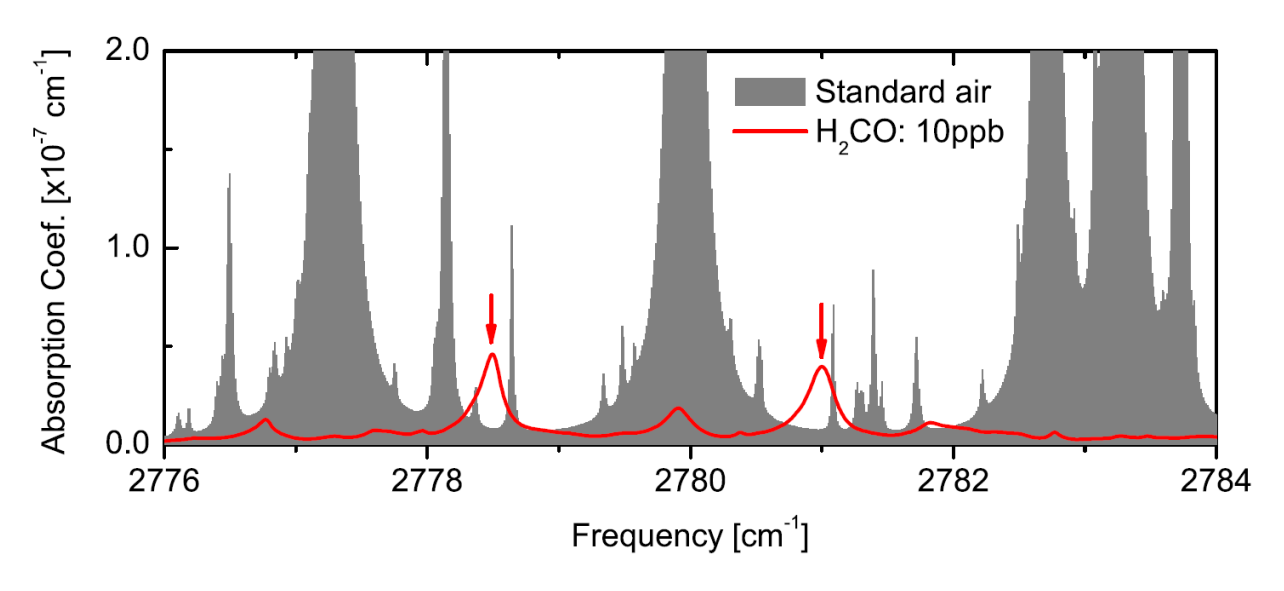


Figure 1. Simulated absorption spectra of standard air (1.86%  $H_2O$ , 327 ppm  $CO_2$ ,30 ppb  $O_3$ , 320 ppb  $N_2O$ , 150 ppb CO, 1.68 ppm  $CH_4$ , 20.7%  $O_2$ , and 77.4%  $N_2$ ) mixed with 10 ppb  $H_2CO$  at 296 K and 1 atm using the HITRAN database [37].

The recent availability of ICLs with wavelengths between 3–4 μm enables the sensitive detection of trace gases such as formaldehyde (H2CO) that possesses a strong absorption band in this particular wavelength spectral region [25]. A Nanoplus<sup>TM</sup> CW, TEC ICL operating at the wavelength  $\sim$ 3.6  $\mu$ m was selected as the laser source for H<sub>2</sub>CO detection. The ICL performance of laser wavelength and power were first tested and characterized using a Thermo-Fisher<sup>™</sup> Fourier transform infrared (FTIR) spectrometer with a resolution of 0.125 cm<sup>-1</sup> and an optical power meter (Ophir<sup>™</sup>), respectively. Fig. 2(a) shows the wavelength tuning performance of the selected Nanoplus™ ICL. This ICL covers a wavelength range of 2776 to 2784 cm<sup>-1</sup> by tuning its injection current between 22 and 58 mA and temperature between 30 and 40°C. The ICL's output wavelength is nearly linearly proportional to the applied current at a fixed temperature, resulting in a current tuning coefficient of -0.139 cm<sup>-1</sup>/mA. Similarly, the temperature tuning coefficient is determined to be -0.26 cm<sup>-1</sup>/ $^{\circ}$ C for the current and temperature operational range. Hence, the two H<sub>2</sub>CO diagnostic features centered at 2778 cm<sup>-1</sup> and 2781 cm<sup>-1</sup> can be accessed by this ICL as indicated by the grey lines depicted in Fig. 2(a). Fig. 2(b) presents the ICL output power in the current range from 22 to 58 mA at different temperatures. A maximum ICL output power of 4.3 mW can be achieved with an injection current of 58 mA and laser temperature of 30 °C. It should be noted that at a current of ~50 mA, the ICL output power is 4 mW at 30 °C, which is sufficient for most optical sensing applications.

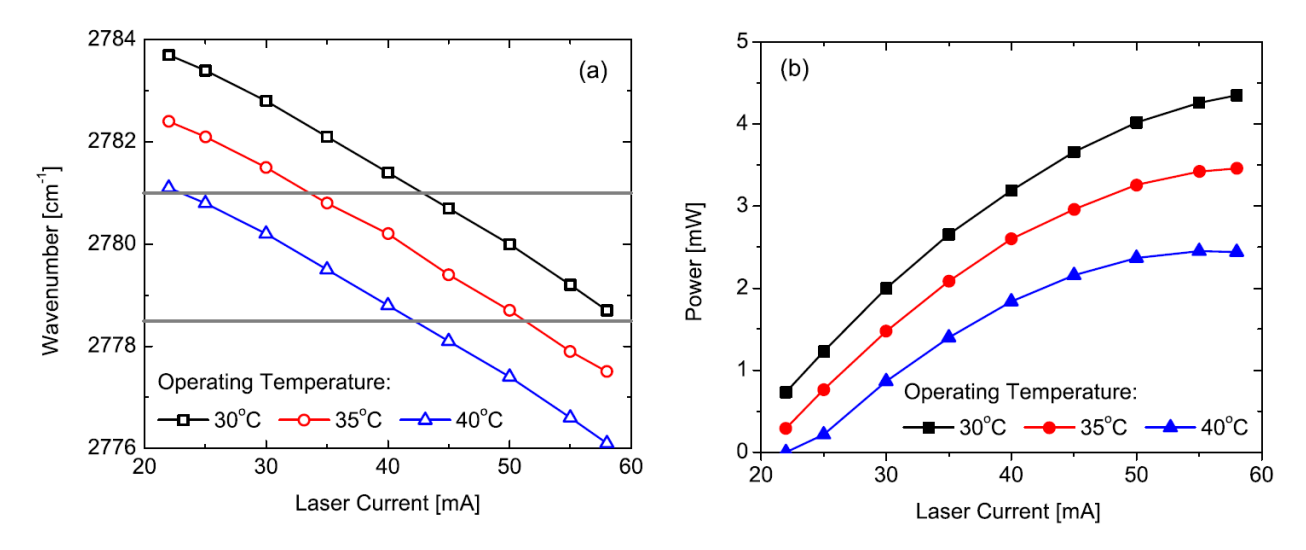


Figure 2. Characterization of the ICL (a) wavenumber and (b) output power as a function of laser injection current.

#### 2.3 Sensor configuration

In trace gas sensing, many sensing techniques such as multipass cell [38], cavity ring-down spectroscopy [39], and integrated cavity output spectroscopy [40] are utilized to achieve the lowest detectable gas concentrations by increasing the effective optical path length. In this work, a novel multipass absorption cell combined with a WMS detection strategy was utilized to enhance the  $H_2CO$  detection sensitivity.

The experimental setup of the multipass cell based  $H_2CO$  sensor is schematically depicted in Fig. 3. The CW ICL housed in a TO66 mount was used as the monochromatic light source emitting at  $\sim$ 3.6  $\mu$ m. The ICL current and temperature were both controlled by a low noise current source (ILX Lightwave) and a high precision temperature controller (Wavelength Electronics, MPT10000), respectively. A visible diode laser beam ( $\lambda$  = 630 nm) was aligned collinear with the mid-infrared beam by means of a dichroic mirror (ISP Optics<sup>TM</sup>, model BSP-DI-25-3) to assist in the optical alignment of the sensor system. The ICL beam was coupled into a novel multipass absorption cell (Sentinel Photonics<sup>TM</sup>, now Aeris Technologies<sup>TM</sup>) using a ZnSe lens of 100-mm focus length. This dense patterned multipass cell consisted of two spherical mirrors separated by a distance of 7.6 cm, providing a sampling volume of 32 ml. By adjusting the distance and relative angle of the axis between two mirrors, dense spot patterns as shown in Fig. 3 can be achieved to provide an effective path length of 3.75 m [41]. The spot pattern covers more of the mirror surface compared to a standard Herriott cell with a simple circle or elliptical pattern.

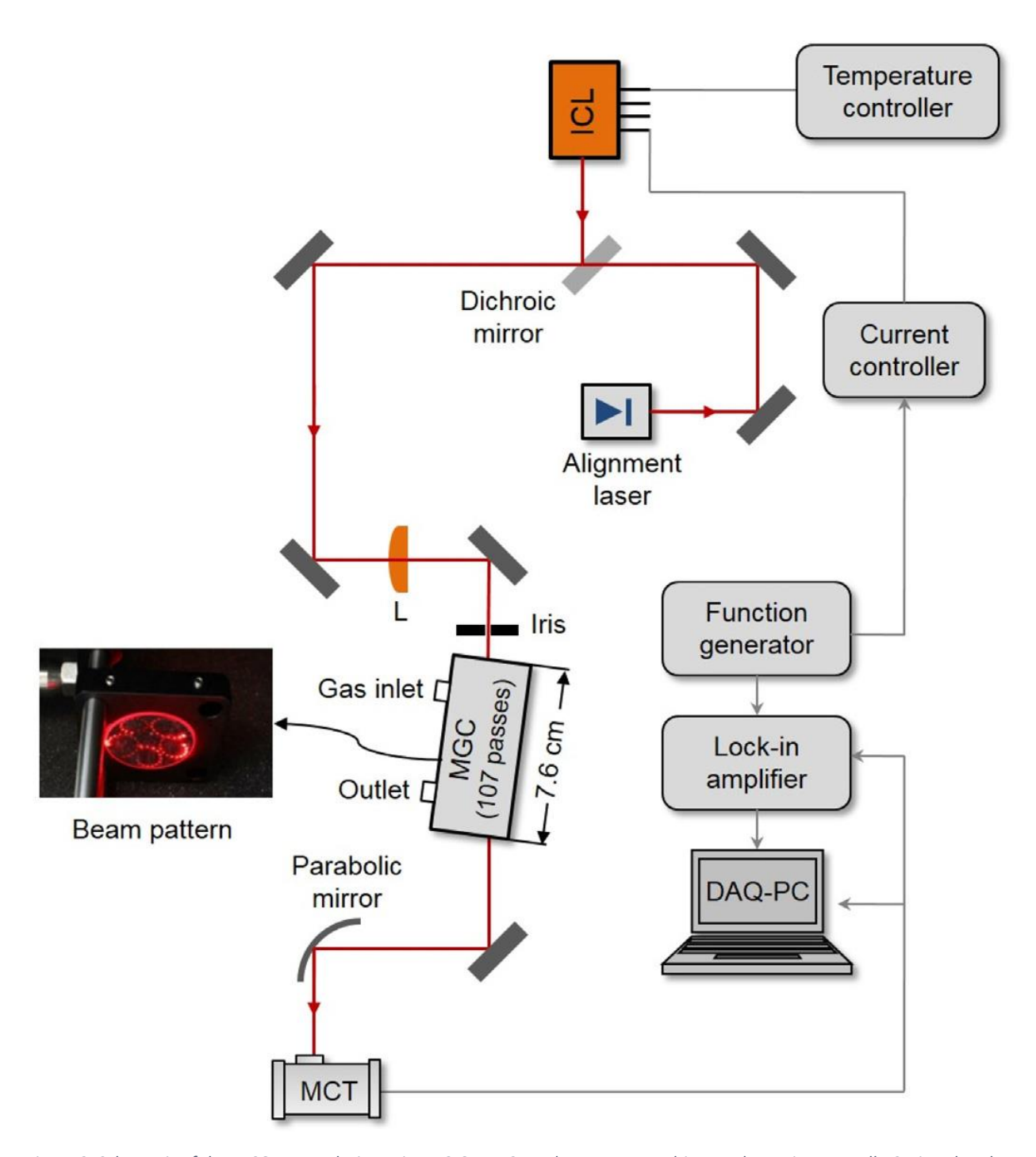


Figure 3. Schematic of the  $H_2CO$  sensor design using a 3.6  $\mu$ m ICL and a compact multi-pass absorption gas cell. ICL, interband cascade laser; MGC, multipass gas cell; MCT, mercury cadmium telluride detector.

The ICL beam exiting the compact multipass cell was focused via a parabolic mirror onto a thermoelectrically cooled mercury cadmium telluride (MCT, Vigo) detector, followed by wavelength modulation spectroscopy with second harmonic detection (WMS-2f). In this work, a superposition of a 1 Hz voltage ramp and 5 kHz sinusoidal dither provided by a function generator (Tektronix AFG3022B) was applied to the ICL current driver to scan and modulate the laser frequency across the H<sub>2</sub>CO absorption

features. The detector signal was processed by a lock-in amplifier (Signal Recovery 7265 DSP) to extract its 2f signal and subsequently processed by a NI DAQ card (NI-DAQ-AI-16XE-50, National Instruments).

#### 2. Results and discussion

#### 2.1 System optimization

The sensor response to the  $H_2CO$  absorption was characterized using a stable concentration of  $H_2CO$  in nitrogen mixture obtained from a permeation based gas generator (Kin-Tek Model 491 M). In the Kin-Tek precision gas mixture generation system, the formaldehyde polymer, paraformaldehyde, is sealed inside a tube with a permeable membrane. A small but stable flow (i.e., nanograms-per-minute) of  $H_2CO$  vapor was emitted through the tube wall a ta constant temperature. The emission rate of the tube depends on the physical characteristics of its permeable membrane, as well as the permeability, temperature and partial pressure of the chemical analyte. With the emission rate characterized, immersing the permeation tube in a carefully controlled flow of dilution gas produces a precision trace gas mixture of the analyte. The mixture concentration could be varied by changing the flow rate of the dilution gas. In the reported work, a target concentration of 0.1 ppm is obtained with a stable air flow rate of 250 cc/min at  $60 \,^{\circ}C$ .

The WMS-2f peak height is dependent on the absorption lineshape, which is related to the gas pressure and the laser wavelength modulation depth [30]. Hence, the gas pressure and ICL wavelength modulation depth must be optimized to obtain the maximum WMS signal. The gas pressure inside the multipass cell is controlled by using a pressure controller (MKS, Model 649) and a diaphragm vacuum pump (KNF, type UN816.3 KTP). Fig. 4 depicts the WMS-2f amplitudes of 750 ppb H<sub>2</sub>CO measured at different pressures and modulation depths. The varied modulation depth was attained by adjusting the sinusoidal voltage applied to the laser current controller. In general, the WMS-2f amplitude increases with higher gas pressure as shown in Fig. 4, but reaches a peak value at a specified modulation voltage if the gas pressure is fixed. The corresponding modulation voltage at the WMS-2f peak shifts to a larger value with increasing gas pressure. For example, the WMS-2f signal peaks at a modulation voltage of ~250 mV and a gas pressure of 60 Torr, which corresponds to ~300 mV at 100 Torr and ~350 mV at 200 Torr, respectively. Despite the stronger WMS signal at higher pressures, the gas pressure inside the multipass cell was controlled below 200 Torr in order to eliminate the possible cross-talk absorption interference between H<sub>2</sub>CO and the neighboring H<sub>2</sub>O and CH<sub>4</sub> absorption lines. Hence, an optimized gas pressure of 200 Torr and a modulation voltage of 350 mV were selected in this study for the sensor development.

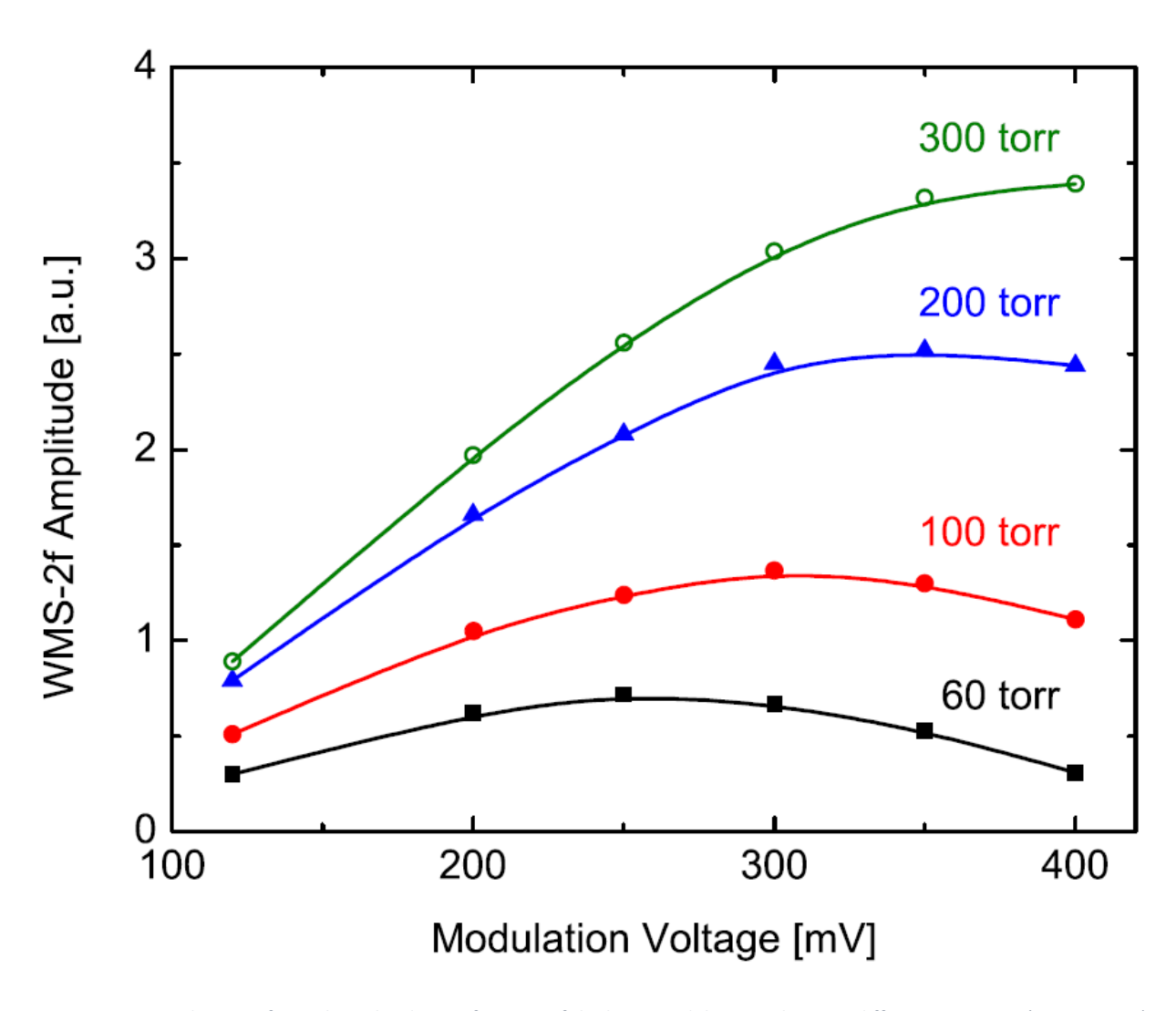


Figure 4. Measured WMS-2f signal amplitude as a function of the laser modulation voltage at different pressures (60–300 Torr).

A typical WMS measurement of  $H_2CO$  absorption is illustrated in Fig. 5. The measurement shown in Fig. 5(a) covers the spectral range between 2778 and 2780.3 cm<sup>-1</sup> for 750 ppb  $H_2CO$  and 1%  $H_2O$  in air at room temperature (296 K) and 200 Torr. Two strong  $H_2CO$  absorption features were observed at 2778.5 and 2779.9 cm<sup>-1</sup>, respectively, despite several  $H_2CO$  lines existing in this wavelength range. The target  $H_2CO$  feature for the present sensor development was centered at 2778.5 cm<sup>-1</sup>, as compared to the other  $H_2CO$  feature at 2779.9 cm<sup>-1</sup> affected significantly by a neighboring  $H_2O$  transition (at 2779.96 cm<sup>-1</sup>). The simulated absorption spectra using the HITRAN database at the same conditions are plotted in Fig. 5(b) for comparison. The simulation agrees well with the experimental results. It should be noted that there exists a  $H_2O$  line centered at 2778.18 cm<sup>-1</sup> and a  $CH_4$  line centered at 2778.64 cm<sup>-1</sup>, which are close to the target  $H_2CO$  feature. The influence of the  $H_2O$  and  $CH_4$  lines on the  $H_2CO$  detection sensitivity will be discussed in Section 3.2.

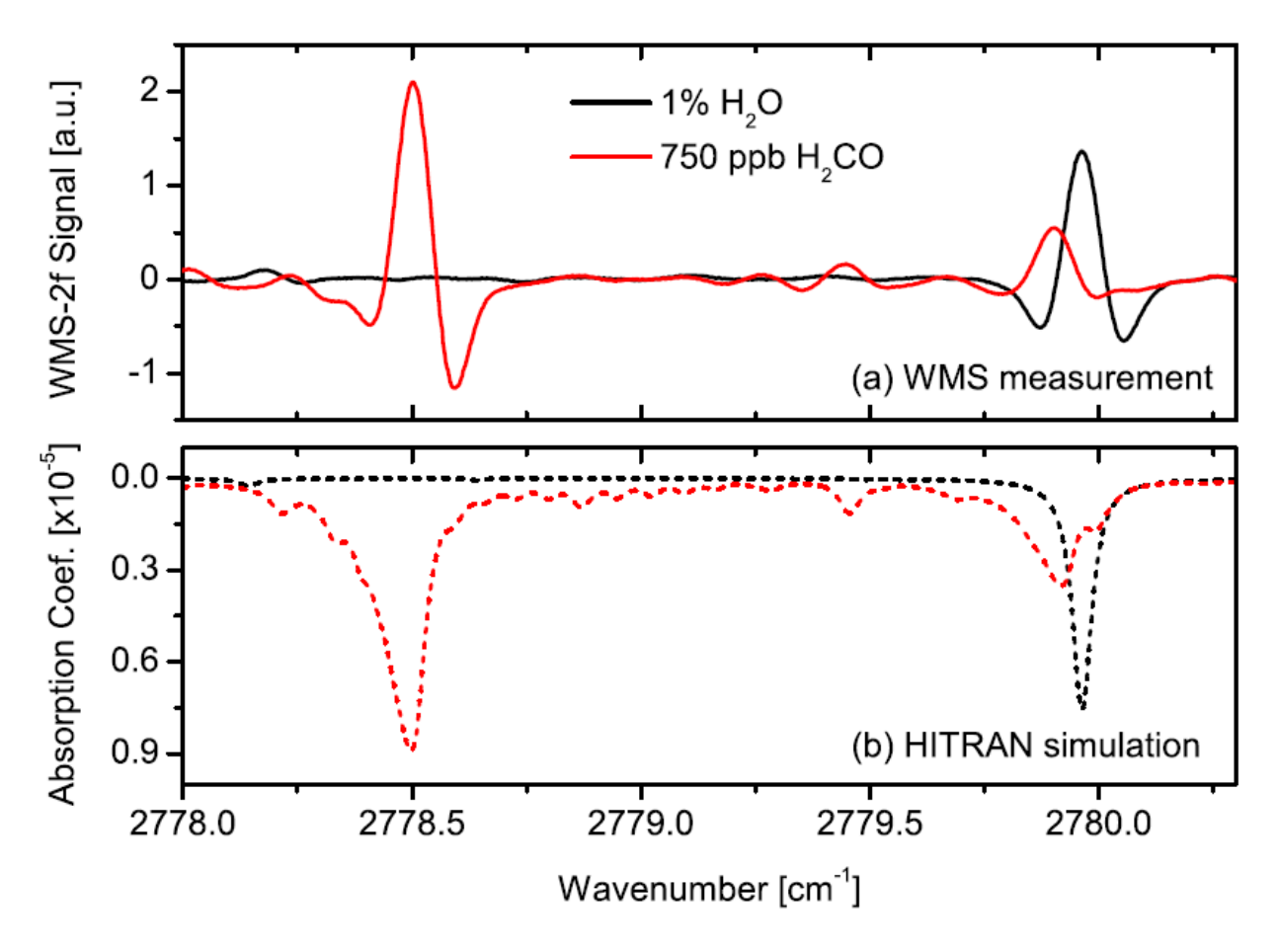


Figure 5. Comparison of (a) the measured WMS-2f signal and (b) simulated absorption coefficient for 750 ppb and 1% H<sub>2</sub>O at 200 Torr. Simulation was performed using the HITRAN database [37].

#### 3.2 Sensor calibration

The sensor calibration was performed using the same experimental setup depicted in Fig. 3 with precision  $H_2CO$  gas mixtures generated from the Kin-Tek permeation gas generator. Two typical WMS-2f profiles measured at the target wavelength of 2778.5 cm<sup>-1</sup> are plotted in Fig. 6, corresponding to calibrated  $H_2CO$  concentrations of 26.8 and 250 ppb, respectively. The relative difference of the detection SNR between these two measurements is clearly seen in Fig. 6. The etalon noise observed when analyzing the  $H_2CO$  mixture with a concentration of 26.8 ppb is mainly due to the interference fringes originating from the multiple reflections between surfaces of optical components, including gas absorption cell, laser, and photodetector. Hence, the implementation of other techniques by angling and antireflection coating of reflective surfaces, asynchronous longitudinal dithering of optical elements, or electronic low pass filtering, can further reduce the amplitude of the etalon fringe signal and thus enhance the detection SNR.

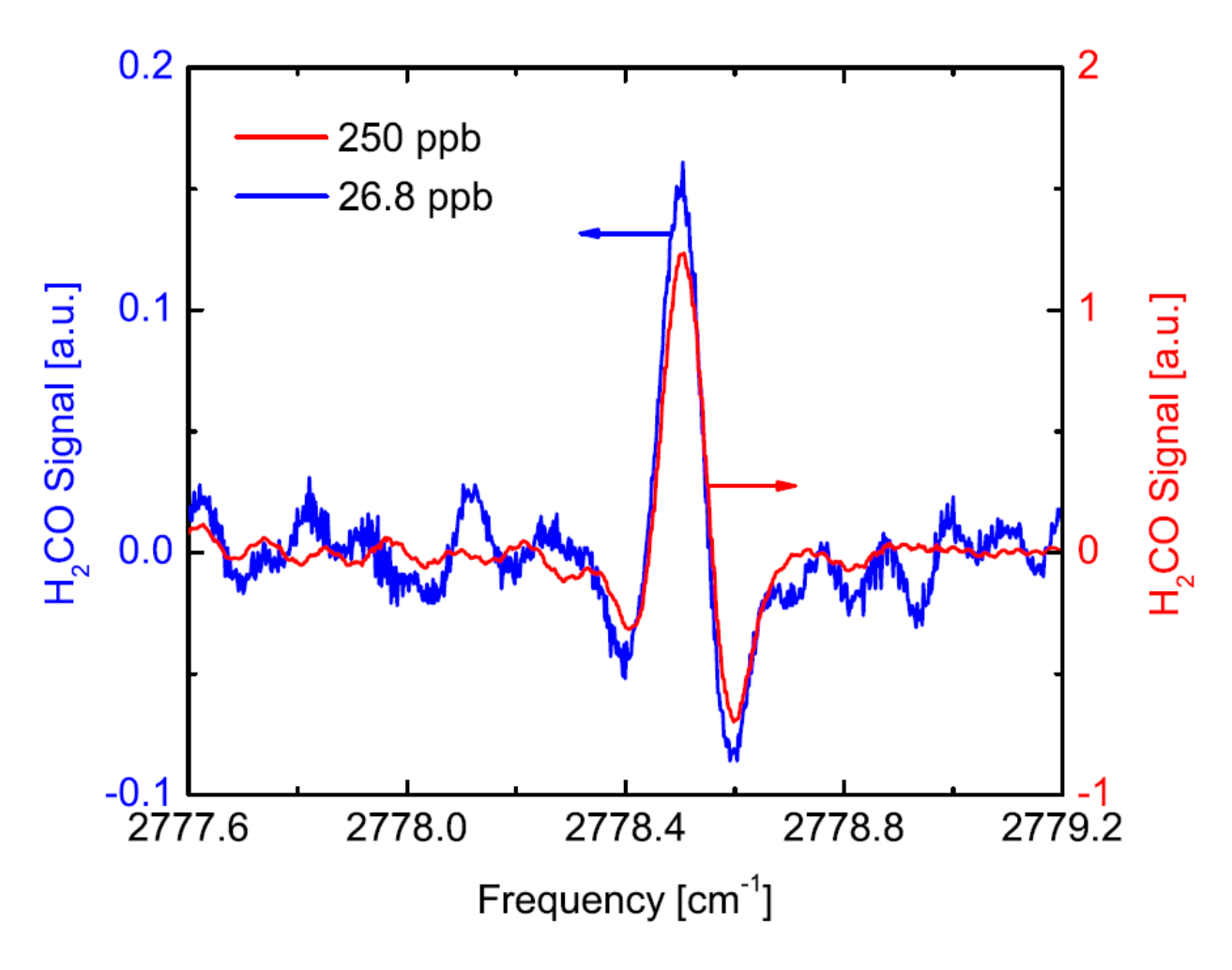


Figure 6. Measured WMS-2f signal of the calibrated  $H_2CO$  mixtures (26.8 ppb and 250 ppb).

The WMS-2f signal was recorded and averaged for ~10 min for each calibrated concentration of the H<sub>2</sub>CO mixture flowing through the multipass gas cell. The experimental results of the measured WMS-2f signal at 2778.5 cm<sup>-1</sup> are plotted in Fig. 7 at different H<sub>2</sub>CO concentrations. The H<sub>2</sub>CO concentration covers a range from 26.8 ppb to 250 ppb to demonstrate the linear response of the sensor system. The coefficient of determination (R-squared value) for linear fitting is 0.997 and the relative difference between the calibrated and the measured H<sub>2</sub>CO concentration based on the determined linear equation is within 8%.

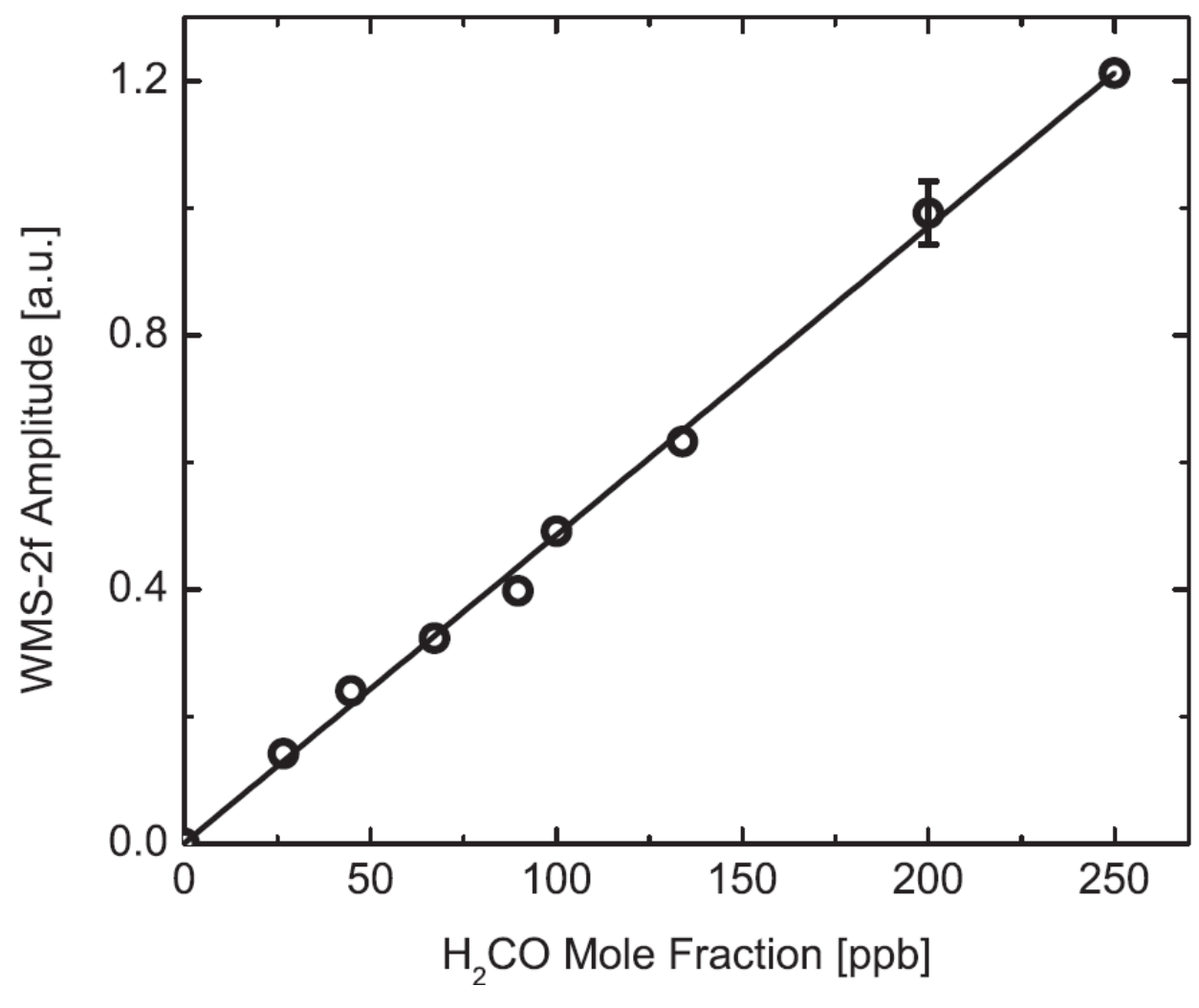


Figure 7. WMS-2f amplitude measured at 2778.5 cm<sup>-1</sup> as a function of  $H_2CO$  concentration. Symbol, measurement; solid line, linear fit (linear fit equation:  $y = 0.00485x + 9.65 \times 10^{-4}$ ).

The detection sensitivity of laser-absorption-based sensors is determined mainly by the overall absorbance, the spectral interference from other gas molecules, and the system noise. We discuss the detection sensitivity according to these three factors.

The spectral interference from neighboring molecular transitions caused by pressure broadening is the first important issue that affects the detection sensitivity in trace gas sensing. A sensitivity simulation was performed using a numerical model to examine the interferences from those two absorption features of H<sub>2</sub>O and CH<sub>4</sub>. The numerical model was constructed based on the mathematical expressions of the WMS-2*f* technique as discussed in Section 2.1 as well as in Refs. [28–32]. The spectroscopic parameters (i.e., line-position, line-strength, and air-broadening coefficient) used in the simulation were obtained from the HITRAN database [37]. An H<sub>2</sub>O absorption line centered at 2778.18 cm<sup>-1</sup> occurs close to the targeted H<sub>2</sub>CO feature at 2778.5 cm<sup>-1</sup> and its potential spectral interference was investigated. Fig. 8(a) shows that the WMS-2*f* spectral simulation of a 10 ppb H<sub>2</sub>CO and a nearby H<sub>2</sub>O absorption line with concentration levels that varied between 0.1% and 2% at a total gas pressure of 200 Torr. In the atmosphere or other gas sensing applications, the H<sub>2</sub>O absorption spans a much larger concentration

range compared to that for  $H_2CO$ . Thus, the  $H_2CO$  con-centration was changed by orders of magnitude in the simulation to demonstrate its influence on the  $H_2CO$  WMS-2f feature. The 2f peak-to-trough height of a 10-ppb  $H_2CO$  peak only decreases by 0.21% as the  $H_2CO$  concentration increases from 0.1% to 2%.

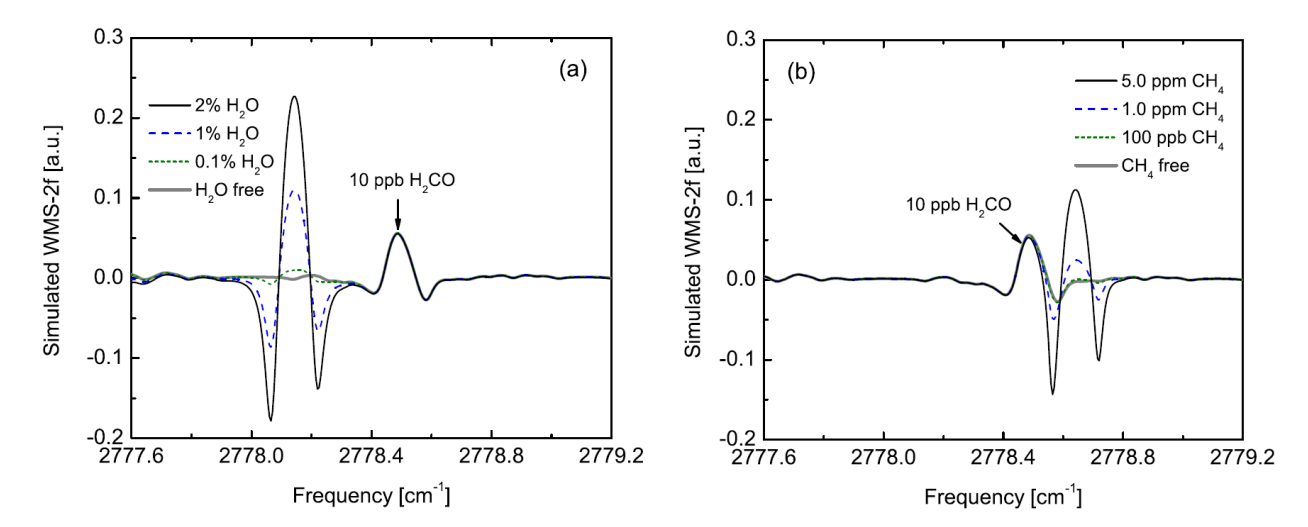


Figure 8. Simulated WMS-2f spectral interferences between 10 ppb  $H_2CO$  and the nearby (a)  $H_2O$  with concentration varied between 0.1% and 2%, and (b)  $CH_4$  with concentration varied between 100 ppb and 5 ppm, at a gas pressure of 200 Torr.

A similar evaluation was performed for the other interfering absorption of  $CH_4$  centered at 2778.64 cm<sup>-1</sup> with concentration levels varied between 100 ppb and 5 ppm, as shown in Fig. 8(b). If the  $CH_4$  present in the gas mixture has a concentration of 1 ppm and 5 ppm, the 2f peak-to-trough height of 10-ppb  $H_2CO$  peak decreases by 1.2% and 5%, respectively. Hence, the interference between these absorption features is insignificant for most atmospheric conditions if the total gas pressure is controlled to be <200 Torr. The spectral cross-talk interference could be further reduced if a lower gas pressure was selected. In addition, the full spectral fitting method also helps to minimize the interference compared to the peak-to-trough signal amplitude adopted in the current study.

The long-term stability and precision of the  $H_2CO$  sensor were tested by monitoring a calibrated 100 ppb  $H_2CO$  mixture for 1 h. Fig. 9 shows an Allan-Werle deviation [42] plot for the 1-h period sampling  $H_2CO$  mixture. The stability of the sensor system in a free running, non-wavelength locked mode allows averaging of up to 140 s for the detection of  $H_2CO$ . A MDL at a sampling rate of 1 Hz was measured to be 6 ppb, based on the absorption line-strength of  $H_2CO$  at this wavelength, a gas pressure of 200 Torr, and an optical path length of 3.75 m. A minimum detection absorption coefficient of  $6.5 \times 10^{-8}$  cm<sup>-1</sup> was achieved using our current sensor configuration. Furthermore, the Allan-Werle deviation shown in Fig. 9 reveals that the MDL can be improved to 1.5 ppb with an integration time of 140 s.

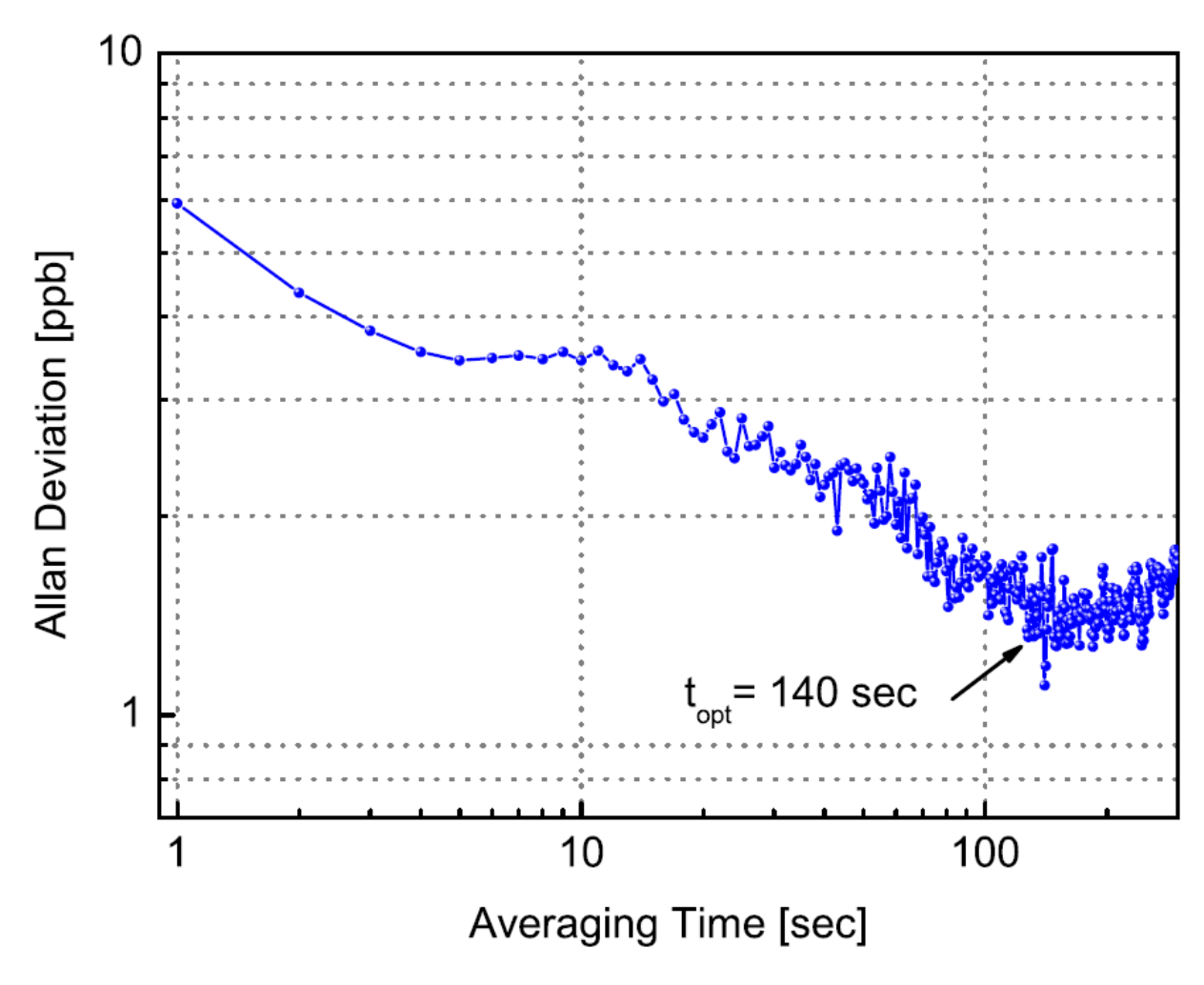


Figure 9. Allan-Werle deviation in ppb of the WMS-2f signal as a function of the averaging time.

#### 4. Conclusion and future outlook

In this paper we have reported the development of a formaldehyde TDLAS sensor using an interband cascade laser at  $\sim 3.6~\mu m$  and a novel multipass absorption gas cell. The low power consumption of the ICL and the compact multipass cell of the sensor system facilitate its convenient field deployment. The absorption interference effects from neighboring  $H_2O$  and  $CH_4$  lines were analyzed in this work and proved to be insignificant if low gas pressures (<200 Torr) were used in the measurement. Wavelength modulation spectroscopy with second harmonic (WMS-2f) detection were used to achieve a 6-ppb MDL of  $H_2CO$  with 1 s averaging time. The long-term stability and precision of this absorption sensor were examined and a 1.5-ppb minimum detectable concentration could be achieved by averaging up to 140 s. Future work is planned to further improve the sensor detectivity to sub-ppb level by using a similar multipass gas cell with longer (54 m) path length. The new sensor system will be installed in a mobile monitoring van for real-time measurements of  $H_2CO$  emissions in the Greater Houston area.

## Acknowledgements

We acknowledge the financial support from a National Science Foundation (NSF) ERC MIRTHE award, a NSF-ANR award for inter-national collaboration in chemistry, "Next generation of Compact Infrared

Laser based Sensor for Environmental monitoring (Nex-CILAS)", and the Robert Welch Foundation grant C-0586. Wei Ren acknowledges financial support from a Direct Grant for Research (C001-4055041) and the Shun Hing Institute of Advanced Engineering (RNE-p2-15, C001-8115052) from The Chinese University of Hong Kong.

#### References

- [1] Y.G. Adewuyi, S.-Y. Cho, R.-P. Tsay, G.R. Carmichael, Importance of formaldehyde in cloud chemistry, Atmos. Environ. 1967. 18 (1984)2413–2420.
- [2] L.G. Anderson, J.A. Lanning, R. Barrell, J. Miyagishima, R.H. Jones, P. Wolfe, Sources and sinks of formaldehyde and acetaldehyde: An analysis of Denver's ambient concentration data, Atmos. Environ. 30 (1996) 2113–2123.
- [3] C. Hak, I. Pundt, S. Trick, C. Kern, U. Platt, J. Dommen, et al., Intercomparison of four different in-situ techniques for ambient formaldehyde measurements in urban air, Atmos. Chem. Phys. 5 (2005) 2881–2900.
- [4] R. Atkinson, Atmospheric chemistry of VOCs and NOx, Atmos. Environ. 34(2000) 2063–2101.[5] M. Lee, B.G. Heikes, D.W. O'Sullivan, Hydrogen peroxide and organic hydroperoxide in the troposphere: a review, Atmos. Environ. 34 (2000)3475–3494.
- [6] Committee on Sick House Syndrome: Indoor Air Pollution Progress Report.No. 4, Japan., (2002).
- [7] S.E. Ebeler, A.J. Clifford, T. Shibamoto, Quantitative analysis by gas chromatography of volatile carbonyl compounds in expired air from mice and human, J. Chromatogr. B. Biomed. Sci. App. 702 (1997) 211–215.
- [8] J.O. Levin, K. Andersson, R. Lindahl, C.A. Nilsson, Determination of sub-part-per-million levels of formaldehyde in air using active or passive sampling on 2,4-dinitrophenylhydrazine-coated glass fiber filters and high-performance liquid chromatography, Anal. Chem. 57 (1985) 1032–1035.
- [9] J.R. Hopkins, T. Still, S. Al-Haider, I.R. Fisher, A.C. Lewis, P.W. Seakins, A simplified apparatus for ambient formaldehyde detection via GC-pHID, Atmos. Environ. 37 (2003) 2557–2565.
- [10] C.-Y. Lee, C.-M. Chiang, Y.-H. Wang, R.-H. Ma, A self-heating gas sensor with integrated NiO thin-film for formaldehyde detection, Sens. Actuators B Chem.122 (2007) 503–510.
- [11] J. Wang, P. Zhang, J.-Q. Qi, P.-J. Yao, Silicon-based micro-gas sensors for detecting formaldehyde, Sens. Actuators B Chem. 136 (2009) 399–404.
- [12] J. Wang, L. Liu, S.-Y. Cong, J.-Q. Qi, B.-K. Xu, An enrichment method to detect low concentration formaldehyde, Sens. Actuators B Chem. 134 (2008)1010–1015.
- [13] M. Hämmerle, E.A.H. Hall, N. Cade, D. Hodgins, Electrochemical enzyme sensor for formaldehyde operating in the gas phase, Biosens. Bioelectron. 11(1996) 239–246.
- [14] Q. Ma, H. Cui, X. Su, Highly sensitive gaseous formaldehyde sensor with CdTe quantum dots multilayer films, Biosens. Bioelectron. 25 (2009) 839–844.

- [15] J.R. Hottle, A.J. Huisman, J.P. DiGangi, A. Kammrath, M.M. Galloway, K.L. Coens, et al., A laser induced fluorescence-based instrument for in-situ measurements of atmospheric formaldehyde, Environ. Sci. Technol. 43 (2009)790–795.
- [16] J.J. Davenport, J. Hodgkinson, J.R. Saffell, R.P. Tatam, Formaldehyde sensor using non-dispersive UV spectroscopy at 340 nm, Proc. SPIE 9141 (2014),91410K–6.
- [17] C.B. Hirschmann, J. Lehtinen, J. Uotila, S. Ojala, R.L. Keiski, Sub-ppb detection of formaldehyde with cantilever enhanced photoacoustic spectroscopy using quantum cascade laser source, Appl. Phys. B 111 (2013) 603–610.
- [18] Y. Mine, N. Melander, D. Richter, D.G. Lancaster, K.P. Petrov, R.F. Curl, et al., Detection of formaldehyde using mid-infrared difference-frequency generation, Appl. Phys. B 65 (1997) 771–774.
- [19] S. Friedfeld, M. Fraser, D. Lancaster, D. Leleux, D. Rehle, F. Tittel, Field intercomparison of a novel optical sensor for formaldehyde quantification, Geophys. Res. Lett. 27 (2000) 2093–2096.
- [20] D.G. Lancaster, A. Fried, B. Wert, B. Henry, F.K. Tittel, Difference-frequency-based tunable absorption spectrometer for detection of atmospheric formaldehyde, Appl. Opt. 39 (2000) 4436–4443.
- [21] D. Rehle, D. Leleux, M. Erdelyi, F. Tittel, M. Fraser, S. Friedfeld, Ambient formaldehyde detection with a laser spectrometer based on difference-frequency generation in PPLN, Appl. Phys. B Lasers Opt. 72 (2001)947–952.
- [22] A. Fried, Tunable diode laser measurements of formaldehyde during the TOPSE 2000 study: Distributions, trends, and model comparisons, J. Geophys.Res. 108 (2003).
- [23] B.P. Wert, Signatures of terminal alkene oxidation in airborne formaldehyde measurements during TexAQS 2000, J. Geophys. Res. 108 (2003).
- [24] J.H. Miller, Y.A. Bakhirkin, T. Ajtai, F.K. Tittel, C.J. Hill, R.Q. Yang, Detection of formaldehyde using off-axis integrated cavity output spectroscopy with an interband cascade laser, Appl. Phys. B 85 (2006) 391–396.
- [25] S. Lundqvist, P. Kluczynski, R. Weih, M. von Edlinger, L. Nähle, M. Fischer, et al., Sensing of formaldehyde using a distributed feedback interband cascade laser emitting around 3493 nm, Appl. Opt. 51 (2012)6009–6013.
- [26] P. Gorrotxategi-Carbajo, E. Fasci, I. Ventrillard, M. Carras, G. Maisons, D.Romanini, Optical-feedback cavity-enhanced absorption spectroscopy with a quantum-cascade laser yields the lowest formaldehyde detection limit, Appl.Phys. B 110 (2013) 309–314.
- [27] A. Perrin, D. Jacquemart, F. Kwabia Tchana, N. Lacome, Absolute line intensities measurements and calculations for the 5.7 and 3.6  $\mu$ m bands of formaldehyde, J. Quant. Spectrosc. Radiat. Transf. 110 (2009) 700–716.
- [28] P. Kluczynski, Å.M. Lindberg, O. Axner, Background Signals in Wavelength-Modulation Spectrometry with Frequency-Doubled Diode-Laser Light. I. Theory, Appl. Opt. 40 (2001) 783–793.
- [29] P. Kluczynski, Å.M. Lindberg, O. Axner, Background signals in wavelength-modulation spectrometry by use of frequency-doubled diode-laser light. II. Experiment, Appl. Opt. 40 (2001) 794.

- [30] P. Kluczynski, O. Axner, Theoretical description based on Fourier analysis of wavelength-modulation spectrometry in terms of analytical and background signals, Appl. Opt. 38 (1999) 5803–5815.
- [31] G.B. Rieker, J.B. Jeffries, R.K. Hanson, Calibration-free wavelength-modulation spectroscopy for measurements of gas temperature and concentration in harsh environments, Appl. Opt. 48 (2009) 5546–5560.
- [32] H. Li, G.B. Rieker, X. Liu, J.B. Jeffries, R.K. Hanson, Extension of wavelength-modulation spectroscopy to large modulation depth for diode laser absorption measurements in high-pressure gases, Appl. Opt. 45 (2006)1052–1061.
- [33] L.R. Brown, R.H. Hunt, A.S. Pine, Wavenumbers, line strengths, and assignments in the Doppler-limited spectrum of formaldehyde from 2700 to 3000 cm<sup>-1</sup>, J. Mol. Spectrosc. 75 (1979) 406–428.
- [34] V. Catoire, F. Bernard, Y. Mébarki, A. Mellouki, G. Eyglunent, V. Daële, et al., A tunable diode laser absorption spectrometer for formaldehyde atmospheric measurements validated by simulation chamber instrumentation, J. Environ.Sci. 24 (2012) 22–33.
- [35] J. Li, U. Parchatka, H. Fischer, Formaldehyde trace gas sensor based on a thermoelectrically cooled CW-DFB quantum cascade laser, Anal. Methods 6(2014) 5483–5488.
- [36] G.W. Harris, G.I. Mackay, T. Iguchi, L.K. Mayne, H.I. Schiff, Measurements of formaldehyde in the troposphere by tunable diode laser absorption spectroscopy, J. Atmospheric Chem. 8 (1989) 119–137.
- [37] L.S. Rothman, I.E. Gordon, A. Barbe, D.C. Benner, P.F. Bernath, M. Birk, et al., The HITRAN 2008 molecular spectroscopic database, J. Quant. Spectrosc. Radiat. Transf. 110 (2009) 533–572.
- [38] D. Herriott, H. Kogelnik, R. Kompfner, Off-axis paths in spherical mirror interferometers, Appl. Opt. 3 (1964) 523–526.
- [39] A. O'Keefe, D.A.G. Deacon, Cavity ring-down optical spectrometer for absorption measurements using pulsed laser sources, Rev. Sci. Instrum. 59(1988) 2544–2551.
- [40] A. O'Keefe, Integrated cavity output analysis of ultra-weak absorption, Chem. Phys. Lett. 293 (1998) 331–336.
- [41] S. So, D. Thomazy, Multipass Cell Using Spherical Mirrors While Achieving Dense Spot Patterns, US20120242989 A1, 2012.
- [42] P. Werle, R. Mücke, F. Slemr, The limits of signal averaging in atmospheric trace-gas monitoring by tunable diode-laser absorption spectroscopy(TDLAS), Appl. Phys. B 57 (1993) 131–139.